High temperature gradient micro-sensors array for flow separation detection and control

Cécile Ghouila-Houri, Abdelkrim Talbi, Romain Viard, Quentin Gallas, Eric Garnier, Alain Merlen, Philippe Pernod

High temperature gradient micro-sensors array for flow separation detection and control

Cécile Ghouila-Houri[1,2], Abdelkrim Talbi[1], Romain Viard[3], Quentin Gallas[2], Eric Garnier[4], Alain Merlen[1], Philippe Pernod[1]

[1] Univ. Lille, CNRS, Centrale Lille, Yncréa ISEN, Univ. Polytechnique Hauts-de-France, UMR 8520 - IEMN, F-59000 Lille, France
[2] Univ. Lille, CNRS, ONERA, Arts et Metiers ParisTech, Centrale Lille, FRE 2017, Laboratoire de Mécanique des fluides de Lille – Kampé de Fériet, F-59000 Lille, France
[3]Fluiditech, Thurmelec, Pulversheim, 68840, France
[4] DAAA, ONERA The French Aerospace Lab, Meudon, 92190, France
E-mail: cecile.ghouila@centralelille.fr ; abdelkrim.talbi@univ-lille.fr

Received xxxxxx
Accepted for publication xxxxxx
Published xxxxxx

Abstract

This paper reports the use of an array of calorimetric micro-sensors that perform bidirectional measurement of wall shear stress, for flow separation detection and control. The sensors design is hot-wire like with three parallel micro wires suspended over a micro-cavity and mechanically supported using periodic perpendicular micro-bridges. The micro-sensors were implemented on a flexible packaging and characterized in a turbulent boundary layer wind tunnel on a flat plate. An array of twelve micro-sensors were then implemented in a flap model designed for active flow control experiments and equipped with pulsed jet actuators. The work included the design and manufacturing of appropriate miniaturized electronics. Without control, the micro-sensors successfully detected the natural flow separation and the flow separation point moving from the trailing edge to the leading edge as the angle of the flap increased. Finally, the micro-sensors characterized the efficiency of the active flow control for avoiding separation.

Keywords: MEMS sensors array, Wall shear stress sensors, Thermal sensors, Calorimetric sensors, Flow control, Flow separation

1. Introduction

One of the main objectives in research on future vehicles concerns the reduction of fuel consumption and CO_2 or toxic NO_x gases emissions. A solution consists in improving the vehicles aerodynamic performances by means of flow control. MacMynowski and Williams [1] defined flow control as a modification of the natural state of the flow to a wanted state. It consists in manipulating free stream or wall bounded flows, using active or passive devices, in order to produce favourable changes in the flow such as preventing separation, delaying laminar-turbulent transition, reducing noise or enhancing mixing. Flow control is thereby a technical solution for both safety and environmental issues.

Boundary layer separation is a mostly unwanted phenomenon for many vehicle related applications and even dangerous in aeronautics. Separation occurring over flaps is indeed responsible for large performance losses especially during take-off as it simultaneously drastically increases drag and reduces lift [2,3]. Passive and active devices have been manufactured to encounter this phenomenon but only active closed-loop control enables to adapt the control to the configuration (take-off, landing and cruise are three different examples of configurations for an airplane) and external

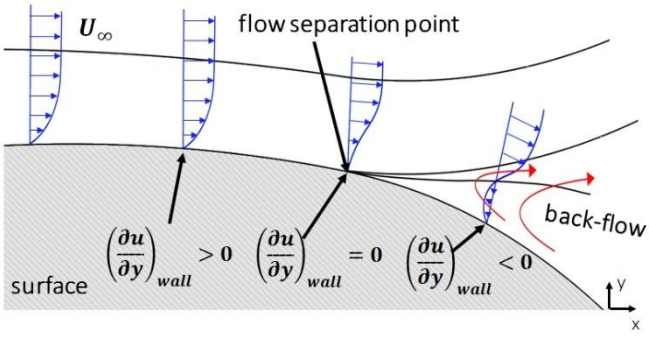

Figure 1. Schematic of flow separation

perturbations (crosswind, vehicle overtaking, etc.). Closed-loop control indeed considers electrically commanded actuators for manipulating the flow, and a set of sensors indicating the state of the flow and used to adapt the actuator control [3]. More precisely, wall shear stress sensors are required as wall shear stress is a key-element in wall turbulence equations.

The wall shear stress τ is proportional to the velocity gradient at the wall and in 2D-flows, it is given by equation (1):

$$\tau = \mu \cdot (\partial u/\partial y)_{wall} \quad (1)$$

where μ is the air dynamic viscosity, u is the flow velocity parallel to the wall, and y is the axis normal to the wall. Flow separation can be characterized by wall shear stress, as shown in Figure 1. An attached flow is indeed characterized by a mean positive shear stress. When a flow is separated, there is a recirculation area, where the shear stress is negative (change of flow direction). The point of separation is the limit between the two states and is characterized by a shear stress equal to zero. A separated flow can also be qualitatively characterized by the wall shear stress fluctuations as they increase sharply when the flow separates [4].

Therefore, accurate time-resolved wall shear stress measurement is crucial for implementing a closed-loop control of separation. Flows at moderate Reynolds numbers exhibits typical length scales of 100 μm at the wall or less and time-scales require several kilohertz of bandwidth [5]. Micro-electro-mechanical systems (MEMS) are thereby a technical solution to resolve turbulent flows.

Micro machined wall shear stress sensors are usually divided into two groups depending on their measurement techniques: direct techniques using floating element devices [6,7] and indirect measurement such as thermal anemometry [5,8]. Löfdahl and Gad-El-Hak [9] presented a review on MEMS based shear stress sensor and discuss the advantages and drawbacks of each techniques. It has to be noted that in most literature papers, the devices are calibrated in a flat plate configuration in wind, but just a few papers used the MEMS sensors to characterize complex flows like separation. For instance, Jiang et al [10] mounted an array of MEMS hot-films on a cylinder for detecting separation. Later, on the same research team, Xu et al [11] integrated an array of MEMS hot-film sensors on a semi-cylindrical aluminium bloc whose angle of attack is changed. The array successfully detected the flow separation point. Leu et al [4] studied a pitching wind turbine blade equipped with 25 MEMS hot-films. All of them detected separation by mean values of output voltage but they needed the RMS value to get more precision. Indeed, their hot-film technology only detected the amplitude of shear stress and not the sign and the sharp peak of RMS value was more accurate for detecting the point of separation.

A last example could be the study of Buder et al [12] in which the flow separation on an airfoil model was characterized using wall mounted double hot-wire micro-sensors. With two hot-wires mounted close one to the other, the work successfully detected separation on the airfoil model using differential measurements. No information on dynamic responses of the sensors regarding separation was given in this work, neither the possibility of closed loop flow control.

In this paper, micro machined wall shear stress micro-sensors based on both thermal anemometry and calorimetric principle are reported along with their utilization for flow separation control application, and more precisely aiming closed-loop separation control. Based on an unconventional thermal microstructure [13,14], the micro-sensors enable the measurement of bidirectional wall shear stress in aerodynamic flows. The purpose of this work is to use an array of such micro-sensors for detecting flow separation on a flap model and characterizing flow separation control.

The first part of the paper introduces the micro-sensors design whose technology was published in previous works [14–16]. The second part is devoted to characterizations in a turbulent boundary layer wind tunnel. Then, the third part presents the implementation of an array of twelve calorimetric micro-sensors for equipping a flap model, with miniaturized electronics. Given the complex geometry of the model and the necessity for smooth surface integration, both the micro-sensors and the miniaturized electronics were embedded on a flexible package. The final part of the paper presents and discusses the flow separation detection and control on the flap model using the array of micro-sensors as measurement devices.

2. Presentation of the thermal micro-sensor

The micro-sensors at stake in this paper are based on both thermal anemometry and calorimetric principle. They are composed of an electrically heated micro-wire, called a heater, and two cold-wires placed on both sides. The central wire is devoted to the indirect measure of wall shear stress using thermal anemometry. It measures indeed the forced convection heat transfer from the hot-wire to the fluid. More precisely, the heat transfer is due to the interaction between

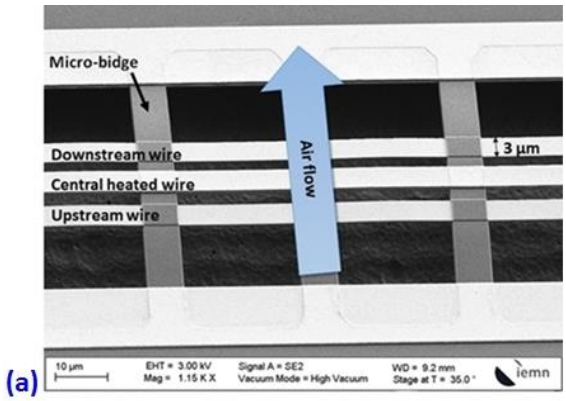

Figure 2. (a) SEM image focused on the HTGC micro-sensor sensitive part along with legend and schematic (b) Integration of the micro-sensor on a flexible package

the thermal boundary layer around the hot-wire and the velocity gradient at the wall, as the transducer is mounted in the wall. Electronic reaction on the heating current allows the hot-wire to work in constant temperature mode and therefore. The two lateral wires, identical in dimensions and materials, are symmetrically heated by the central hot-wire. The flow direction breaks the thermal boundary layer symmetry and the upstream lateral wire is more cooled than the downstream one (Fig. 2 (a)). This principle is called calorimetric. Coupling both principles, the micro-sensors are able to measure the wall shear stress amplitude and sign. This property gives a direct advantage for flow separation detection, as this phenomenon is characterized by both a diminution of the wall shear stress amplitude and an inversion of its sign.

The micro-sensors sensitive part is composed of three parallel micro-wires whose dimensions are 1 mm long, 3 µm wide and less than 1 µm thick (330 nm for the lateral wires and 730 nm for the central wire). The lateral wires are composed of a SiO_2 layer for mechanical support and a Ni/Pt multilayer forming the metallic measurement wire. The central hot-wire is engineered with multiple layers including SiO_2, a Ni/Pt multilayer, another layer of SiO_2 and an Au layer. The heating current crosses the Au layer and the Ni/Pt multilayer thermistors used for measurement. Contrary to conventional designs of hot-wire and hot-film sensors for which the heater is used for measurements, this microstructure uncouples heating and measure and built-on purpose electronics were therefore developed. The micro-wires are separated from the substrate over a 20 µm deep cavity for avoiding thermal losses by conduction in the substrate and enhancing heat transfer by convection with the fluid.

As the maximum working temperature of the micro-sensors is 90°C, radiation can be neglected in the heat transfer mechanism, and then the whole heat transfer measured by the thermal micro-sensor is due to the interaction between the thermal boundary layer and the fluid boundary layer. Suspended periodic perpendicular micro-bridges are disposed along the wire length for mechanical support (Fig. 2 (a)).

The fabrication process uses microtechnology techniques and includes seven main steps that are presented in details in [15]. The micro-sensors, with front-side contacts, are welded on a flexible packaging (Fig. 2 (b)).

3. Characterizations in turbulent boundary layer

The micro-sensors were characterized in a turbulent boundary layer as published in [16]. The wind tunnel used for experiments has a 30 cm × 30 cm test section and nominal free-stream velocity U_∞ goes up to about 35 m/s. The micro-sensor was integrated in the wall of the wind tunnel, at a position where the mean flow was two-dimensional as measured using a hot-wire probe (Dantec 55P11).

We characterized the micro-sensors the same way as it was done in [16] by evaluating their response to wall shear stress variation.

We first indirectly evaluated the wall shear stress variation with the flow velocity. For that, we characterized the boundary layer from 10 m/s and 35 m/s using hot-wire probe to measure the flow velocity in the boundary layer and deduce its thickness $\delta = 19$ mm.

We could calculate the momentum thickness θ from each velocity profile (equation 2).

$$\theta = \int_0^{\delta} \frac{u(x,y)}{U_\infty(x)} \left(1 - \frac{u(x,y)}{U_\infty(x)}\right) dy \qquad (2)$$

The relation of Coles-Fernholz in the equation (3) gave then the skin friction coefficient C_f[17]. The wall shear stress τ was finally deduced from relation (4) as a function of C_f and U_∞. This method links the hot-wire measurements at the center of the wind tunnel test section with the shear stress or the wall velocity.

$$C_f = 2\left(\frac{1}{k}\ln Re_\theta + C\right)^{-2} \qquad (3)$$

with $k = 0.384$, $C = 4.127$,

$$\tau = \frac{1}{2}\rho U_\infty^2 C_f \qquad (4)$$

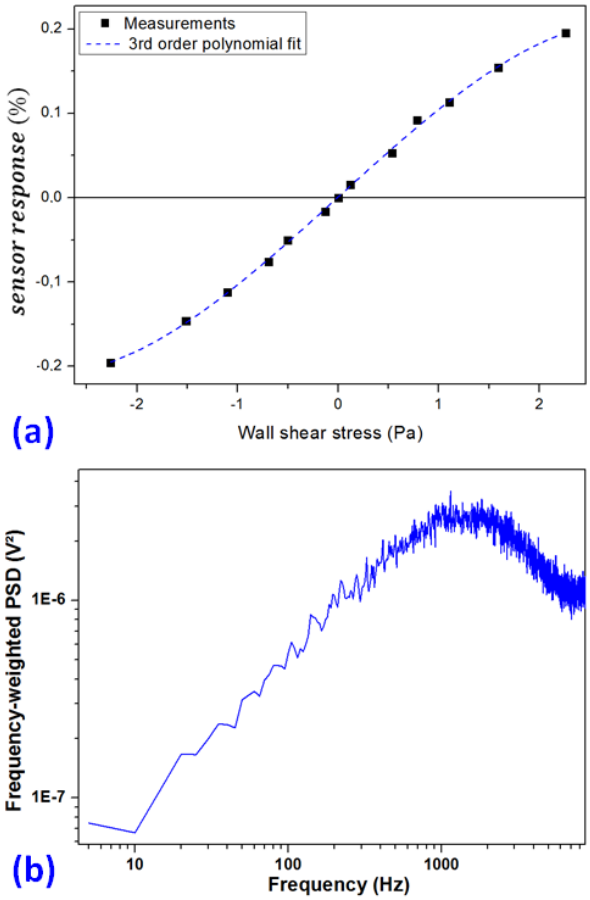

Figure 3. (a) Characterization of the micro-sensor in the package used for the implementation on models (b) Frequency-weighted power spectral density (PSD) measured for $\tau = 2.2$ Pa with the same package

The package used for implementation on models, with front side contacts, differs from the one used in [16], which was perfectly flush but fragile. In the present configuration, the micro-sensors are not perfectly flush mounted but in a 100 µm deep cavity. Therefore, the expected calibration curve should present less sensitivity in terms of voltage variation than in the previous work.

The micro-sensor responses are presented in Figure 3 (a) and (b), with the averaged measurement in (a) and the frequency-weighted power spectral density for $\tau = 2.2$ Pa in (b). In (a), the amplitude of the response is measured using the central wire via constant temperature anemometry, and the sign is given by the difference of resistance (equivalent to the difference of temperature) between the two lateral wires. The sensitivity of the micro-sensor is less important as obtained in [16] due to the different package, but it is sensitive enough to fit the classical third-order polynomial curve [5].

We also evaluated the sensor response to wall shear stress fluctuations by measuring the power spectral density (PSD).

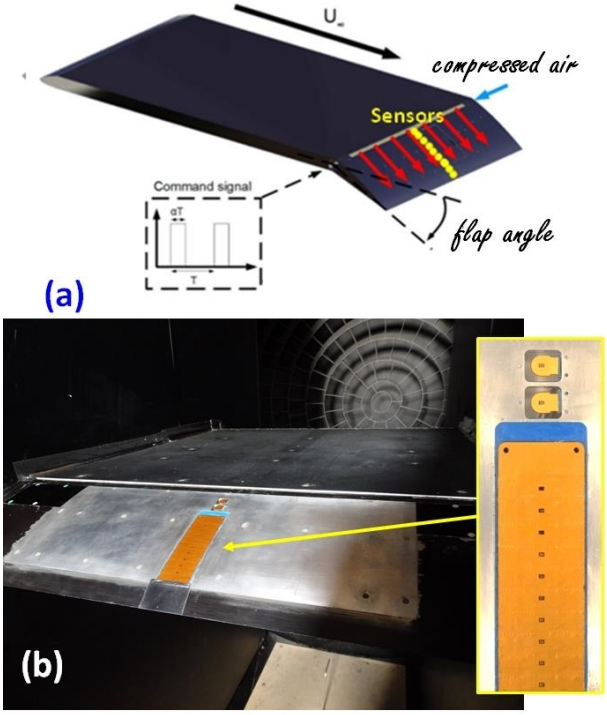

Figure 4. (a) Schematic of the experiment on the flap model (b) Flap model set up in the ONERA L1 wind tunnel and equipped with the array of micro-sensors.

More precisely, the frequency weighted PSD corresponds to the turbulent kinetic energy of the flow. As shown in Figure 3 (b), it is characterized by a hump shape. The interval of frequency centered in the hump is characteristic of the turbulent eddies that transport energy in the flow. The effect of the package is also visible on this response. As shown in Figure 3 (b), the frequency-weighted PSD is damped compared to [16] especially for frequencies higher than 1 kHz. This means that the micro-sensor in this package is blind to the smallest scales of the wall turbulence and underestimates the turbulent kinetic energy present in the boundary layer. These characteristics must be taken into account in the experiments on models, as the sensor measurements will not give all the information about the turbulent spectrum. Nonetheless, such kind of mounting is enough to detect the flow separation while ensuring robustness and implementation possibility.

4. Integration of an array of micro-sensors in a flap model

Flaps are used on airplanes to delay separation during take-off and landing by changing the profile of the wing.

The model used in this study (Fig. 4 (a)) is composed of an 867-mm-long flat-plate and a plain unslotted flap with a chord length of 220 mm. The flap profile was based on a NACA 4412 airfoil shape. It was equipped with an array of micro-sensors as presented above and seven pulsed jet actuators.

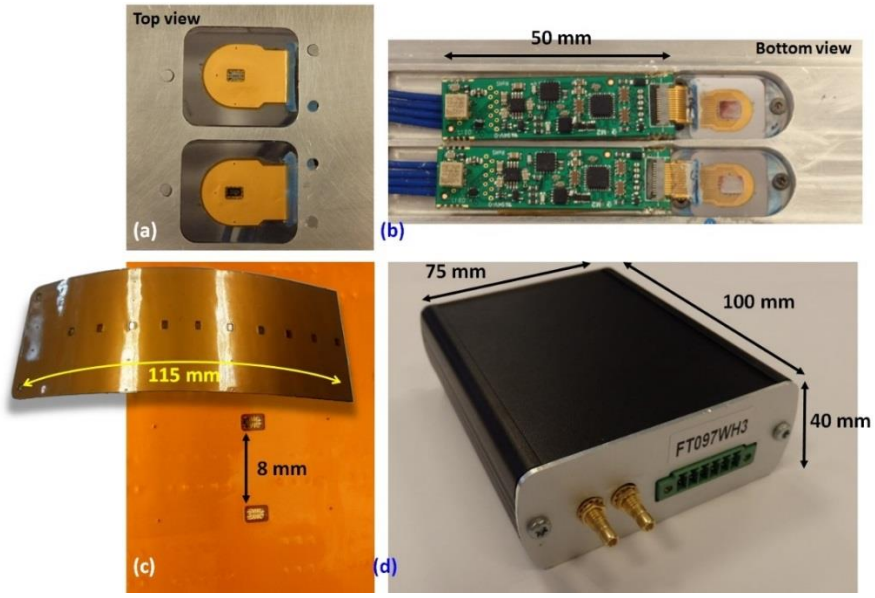

Figure 5. (a) The two leading edge micro-sensors (b) Individual constant-temperature electronics for the leading edge sensors (c) Flexible strip with zoom on two micro-sensors (d) One of the three instrumentation electronics boxes embedded below the flat plate.

The flow control experiments presented in this paper followed the work of Chabert et al [18]. This work studied the natural flow separation occurring on an inclined flap using tomoscopy flow visualizations and commercially available hot-film sensors measurements. With the hot-films, two separation criteria based on higher-order statistical moments (skewness and kurtosis) of signals were proposed to detect flow separation. Open loop control using the Festo MHE2 valves is also demonstrated.

In the present work, the same model was used but the hot-film sensors along the cord were replaced by the calorimetric micro-sensors presented above (Figure 4 (b)) and the flap was machined to allow the integration of the MEMS devices with embedded electronics.
The experiments took place in the large semi-industrial L1 wind tunnel in ONERA Lille. The wind tunnel test section has a diameter of 2.40 m. The flap model was placed between two plates to avoid side effects. Therefore, the mean flow was almost two-dimensional at the center of the flap. The long flat plate is used to stabilize the boundary layer before the flap.

The seven actuators implemented on the flat are Festo MHE2 actuators, same as in Chabert et al [18]. These two-state solenoid valves allow the compressed air flow to blow through 0.25 mm high and 90 mm long slots. The distance between two slots is 7 mm and the distance between the extreme slots and the wall plates is 64 mm. Therefore, 80% of the total flap span is covered.

The twelve micro-sensors were implemented in the flap model in two different kind of integration package, as shown in Figure 4 (b). Two micro-sensors had individual packages as presented in Figure 2 (b), with built-on-purpose CT electronics. They were placed close to the leading edge of the flap. The other ten micro-sensors were mounted on a flexible 3 mm thick strip with shared electronics. This array took place in the thinner part of the model profile and ended 30 mm upstream the trailing edge. Its flexibility allowed following the airfoil profile camber.

Figure 5 shows in (a) a zoom on the leading edge individual micro-sensors and in (b) their miniaturized CT electronics. The micro-sensors electronics was only 3 mm thick and 50 mm long. The micro-sensors were mounted as flush as possible at the flap model surface using PMMA support manufactured for following the flap camber.
Figure 5 (c) shows the 115 mm long flexible strip with a focus on two micro-sensors. There are 10 micro-sensors embedded into the flexible strip, 8 mm away one from the other.
Figure 5 (d) shows an instrumentation box with amplification electronics. Three boxes were needed: one for each individual sensor and one for the strip. The three boxes presented dimensions small enough to be embedded inside the flat plate upstream of the flap.

5. Active flow separation control experiments

We conducted active flow control experiments with two objectives: first, the characterization of the natural flow separation using the micro-sensors array, and second, the characterization of open-loop active flow control using the pulsed jets. These experiments are preliminary to further work focused on closed-loop separation control.

The flow separation is characterized by a negative mean wall shear stress. The first objective was then using the calorimetric micro-sensor to detect the flow separation on the flap model. Given the curvature of the profile, the separation is meant not to appear abruptly but the separation point moves from the trailing edge to the leading edge, as the flap angle increases.

The 12 micro-sensors are meant to detect the moving point of separation. The central wire of each micro-sensor gives the variation of amplitude of the shear stress component perpendicular to the wires, while the lateral wires detected the sign. The combination of both information thus allows the determination of the bonded or separated nature of the flow field on the flap.

Moreover, separation causes a fall in turbulent energy and it therefore can be characterized using the turbulent spectrum (frequency-weighted PSD). This characteristic explains the working of flow control: fluidic actuators are meant to add momentum to the boundary layer to compensate the lack of turbulent energy on a separated flow.

The experiments were conducted at a nominal free-stream velocity $U_\infty = 24.5\ m/s$ corresponding to a Reynolds number based on the chord of $Re_c = 3.45 \times 10^5$.

Figure 6 shows the averaged and normalized by maximum measurements of the voltage variations of three micro-sensors, located respectively in $x/c = 0.3$ (black curve and square symbols), in $x/c = 0.64$ (red curve and round symbols) and in $x/c = 0.86$ (red curve and triangle symbols). The first one was one of the two individual micro-sensors at to the leading edge. The other two were located on the flexible strip.

The first thing to note is the location of the separation point as a function of the flap angle. Thanks to the detection of the sign of the shear stress component perpendicular to the wires, the calorimetric micro-sensors could intrinsically detect separation, which was not the case in the study of Chabert with the hot films. In the work of Chabert et al [18], the flow separation point was deduced by comparing one hot-film response to the ones close to it. A correlation between the hot films was indeed necessary. Detecting the flow direction, the micro-sensors presented in this paper did not need such comparison: they could detect the flow separation by their own, independently one from the other. The correlation was indeed made between the lateral wires of one calorimetric micro-sensor.

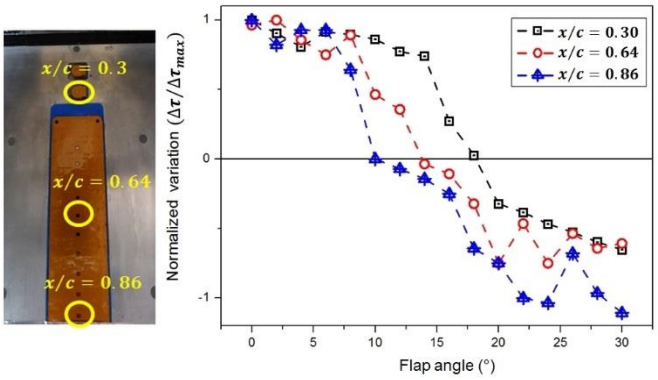

Figure 6. Detection of separation: normalized response of the micro-sensors located at $x/c = 0.3, x/c = 0.64, x/c = 0.86$ for $U_\infty = 24.5\ m/s$.

The three micro-sensors being located at different locations along the chord, the shifting of the separation point as a function of the angle of attack was detected. For $x/c = 0.86$, the separation appeared at an angle of 10°. Then the point of separation went up to appear for 13° at $x/c = 0.64$. Finally, the micro-sensor at $x/c = 0.20$ detected the point of separation at 18°.

Then, active flow control experiments were performed using the Festo MHE2 valves as pulsed jets actuators and the micro-sensors as sensing devices. The pulsed jets worked at 60 Hz with 50 % duty cycle and were supplied by 20 g/s of airflow.

The following results, displayed in Figures 7 and 8, deal with the control of separation, using pulsed jets as actuator devices. When the flow is attached, the goal of flow control is to avoid or at least delay the separation apparition. Here, we did not focus on controlling a separated flow, which aims at reattaching it. All the following results comes from the second individual sensor placed at $x/c = 0.3$, with an upstream velocity $U_\infty = 24.5\ m/s$.

Figure 7 presents the normalized voltage variation of measurements obtained without and with control. The normalization was made using the maximum voltage variation, obtained for 0° with pulsed jets control. It corresponds to the configuration where the maximum shear stress is obtained.

As shown on Figure 7 and previously in Figure 6, the separation at $x/c = 0.3$ occurred for an angle of about 18°, which was detected by the change of sign that is to say, the change of flow direction. On the contrary, with pulsed jets control, the flow direction did not change after 18° of angle, meaning that the shear stress remains positive, and so even at 30° of angle. The flow therefore remained attached to the flap.

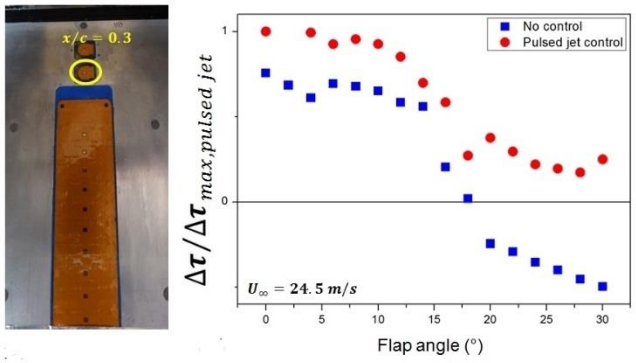

Figure 7. Control of separation: normalized response of the micro-sensor located at $x/c = 0.3$ for $U_\infty = 24.5$ m/s, comparison without and with pulsed jets control

Active flow control successfully controlled separation by avoiding its apparition. At small angles, the voltage variation obtained with pulsed jets was higher than the one obtained without control. This is explained by the sensor position along the chord, close to the actuators, that induced over friction when the flow is naturally attached.

The separation detection and control were also visible with dynamic measurements measuring the power spectral density (PSD) as shown on Figure 8 (a). At 2° and 10°, the flow is attached to the flap for $x/c = 0.3$ and the two PSD are close one to another. At 20°, the flow has just separated and the PSD amplitude starts to attenuate. Finally, at 30°, the flow is fully separated and the spectrum is much damped.
The effect of control appears also in the frequency-weighted PSD. In Figure 8 (b), three spectra are compared: the one obtained at 2° (flow naturally attached), the one at 30° (flow naturally separated) and the one at 30° with pulsed jets. The baseline of this last one reaches an amplitude close to the one for the natural attached flow at 2°. A set of peaks appears due to the pulsed actuation. The main peak is at 60 Hz and corresponds to the pulsed jet frequency; the others are the following harmonics.

The results presented in Figures 6 to 8 demonstrate the performance of the MEMS sensors for separation detection and are promising for implementing a closed-loop control of this phenomenon. In the study of Chabert et al [18] on the same model, the direct measurements from the hot-films were not enough to detect the separation and skewness and kurtosis calculations were needed. Other works, like the ones of Jiang et al [10] and Leu et al [4], needed the RMS value to accurately detect if the flow is separated or not.
The main advantage of the present calorimetric MEMS transducers lies in the direct and accurate detection of separation thanks to the measurement of both the amplitude and sign of the wall shear stress.

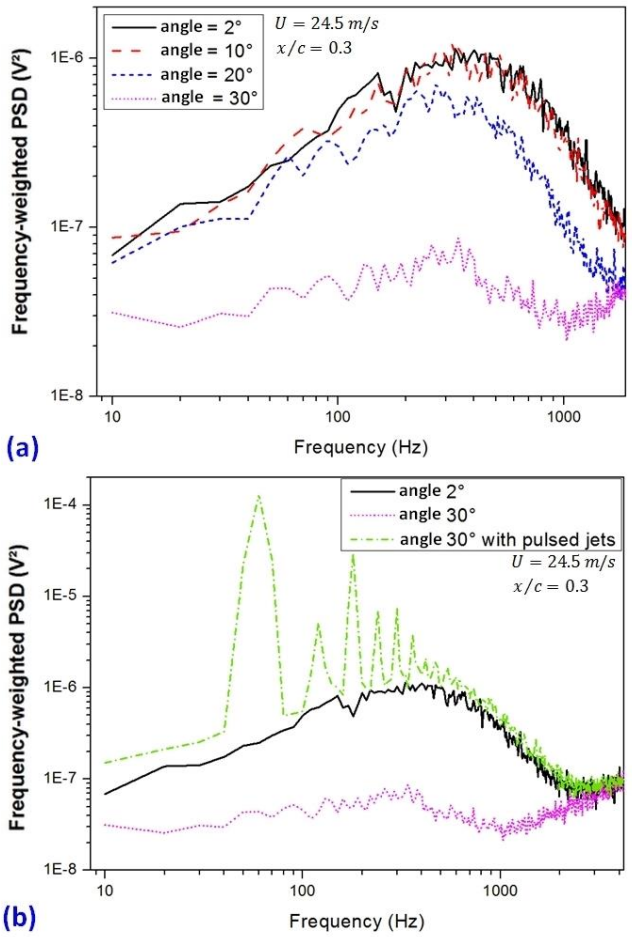

Figure 8. (a) Natural separation on the flap at $x/c = 0.3$ for $U_\infty = 24.5$ m/s: Frequency-weighted Power Spectral Density for 2°, 10°, 20°, 30°. (b) Control of separation: Frequency-weighted Power Spectral Density for 30° with active flow control using pulsed jets

Few studies investigated the use of calorimetric or differential measurements for detection separation. One can cite for instance the work of Buder et al [12] with double-hot-wire MEMS sensors implemented on an airfoil with flap model and the work of Sturm et al [19] who implemented thermoelectric calorimetric sensors on an airfoil like model. Both studies were used to detect separation using differential measurements as done in the present work. However, both of them investigated neither dynamic responses nor active or closed loop control of separation.
The present demonstration of both the detection of separation and the effect of control provides promising preliminary results for implementing closed loop separation control.

6. Conclusion

This paper presented micro machined sensors based on thermal transduction and calorimetric principle and their application for wall shear stress measurement and flow

separation control applications in aeronautics. The main advantages of the micro-sensors compared to conventional sensors lie in the miniaturized dimensions, the integration capability for implementation in models and the simultaneous measurement of wall shear stress amplitude variation and flow direction.

The first part of the paper presented the unconventional design of the micro-sensors along with the calibrations performed in a canonical boundary layer. These experiments demonstrated the ability of the micro-sensors to measure bidirectional wall shear stress after calibration.

The second part was devoted to the presentation of the implementation of twelve micro-sensors with miniaturized electronics into a flap model designed for flow separation control. This part successfully demonstrated the integration of the micro-sensors with build-on purpose electronics in a complex environment.

For future work, we are actually working on improving the electronics to enlarge the bandwidth up to several dozens to hundreds of kilohertz. We also develop a new packaging to improve the signal to noise ratio and avoid damping signals.

The final part of the paper presented the detection of the natural separation on the flap, as the angle of attack increased. Measuring both the variation of amplitude and the variation of sign of wall shear stress, the micro-sensors detected by their own the separation point shifting from the trailing edge to the leading edge. As the flap was also equipped with pulsed jets, open-loop flow control experiments were performed. The micro-sensors successfully detected and characterized the effect of active control. These experimental results are preliminary for future work focused on closed-loop flow control, using the micro-sensors as input for the reaction loop.

Acknowledgements

This work is funded by the French National Research Agency (ANR) in the framework of the ANR ASTRID "CAMELOTT" project. It is supported by the regional platform CONTRAERO in the framework of the CPER ELSAT 2020 project, co-financed by the European Union with the European Regional Development Fund, the French state and the Hauts-de-France Region Council. The authors also thank RENATECH, the French national nanofabrication network, and FEDER.

References

[1] MacMynowski D G and Williams D 2009 Flow Control Terminology Fundamentals and Applications of Modern Flow Control (American Institute of Aeronautics and Astronautics) pp 59–71

[2] Gad-el-Hak M and Bushnell D M 1991 Separation Control: Review J. Fluids Eng **113** 5–30

[3] Gad-el-Hak 2001 Flow Control: The Future Journal of Aircraft **38** 402–18

[4] Leu T S, Yu J M, Miau J J and Chen S J 2016 MEMS flexible thermal flow sensors for measurement of unsteady flow above a pitching wind turbine blade Experimental Thermal and Fluid Science **77** 167–78

[5] Sheplak M, Chandrasekaran V, Cain A, Nishida T and Cattafesta III L N 2002 Characterization of a silicon-micromachined thermal shear-stress sensor AIAA Journal **40** 1099–104

[6] Chandrasekharan V, Sells J, Meloy J, Arnold D P and Sheplak M 2011 A Microscale Differential Capacitive Direct Wall-Shear-Stress Sensor Journal of Microelectromechanical Systems **20** 622–35

[7] Lv H, Jiang C, Xiang Z, Ma B, Deng J and Yuan W 2013 Design of a micro floating element shear stress sensor Flow Measurement and Instrumentation **30** 66–74

[8] Talbi A, Gimeno L, Gerbedoen J-C, Viard R, Soltani A, Mortet V, Preobrazhensky V, Merlen A and Pernod P 2015 A micro-scale hot wire anemometer based on low stress (Ni/W) multi-layers deposited on nano-crystalline diamond for air flow sensing Journal of Micromechanics and Microengineering **25** 125029

[9] Löfdahl L and Gad-el-Hak M 1999 MEMS-based pressure and shear stress sensors for turbulent flows Measurement Science and Technology **10** 665

[10] Jiang F, Lee G-B, Tai Y-C and Ho C-M 2000 A flexible micromachine-based shear-stress sensor array and its application to separation-point detection Sensors and Actuators A: Physical **79** 194–203

[11] Xu Y, Jiang F, Newbern S, Huang A, Ho C-M and Tai Y-C 2003 Flexible shear-stress sensor skin and its application to unmanned aerial vehicles Sensors and Actuators A: Physical **105** 321–9

[12] Buder U, Petz R, Kittel M, Nitsche W and Obermeier E 2008 AeroMEMS polyimide based wall double hot-wire sensors for flow separation detection Sensors and Actuators A: Physical **142** 130–7

[13] Viard R, Talbi A, Merlen A, Pernod P, Frankiewicz C, Gerbedoen J-C and Preobrazhensky V 2013 A robust thermal microstructure for mass flow rate measurement in steady and unsteady flows Journal of Micromechanics and Microengineering **23** 065016

[14] Ghouila-Houri C, Claudel J, Gerbedoen J-C, Gallas Q, Garnier E, Merlen A, Viard R, Talbi A and Pernod P 2016 High temperature gradient micro-sensor for wall shear stress and flow direction measurements Appl. Phys. Lett. **109** 241905

[15] Ghouila-Houri C, Gallas Q, Garnier E, Merlen A, Viard R, Talbi A and Pernod P 2017 High temperature gradient calorimetric wall shear stress micro-sensor for flow separation detection Sensors and Actuators A: Physical **266** 232–41

[16] Ghouila-Houri C, Talbi A, Viard R, Gallas Q, Garnier E, Merlen A and Pernod P 2019 Unsteady flows measurements using a calorimetric wall shear stress micro-sensor Exp Fluids **60** 67

[17] Nagib H, Chauchan K A and Monkewitz P A 2007 Approach to an asymptotic state for zero pressure gradient turbulent boundary layers Philosophical Transaction of the Royal Society **365** 755–70

[18] Chabert T, Dandois J, Garnier E and Jacquin L 2013 Experimental detection of a periodically forced turbulent boundary layer separation Experiments in Fluids **54** 1430

[19] Sturm H, Dumstorff G, Busche P, Westermann D and Lang W 2012 Boundary Layer Separation and Reattachment Detection on Airfoils by Thermal Flow Sensors Sensors **12** 14292–306